QUANTUM LIMITED QUASIPARTICLE MIXERS AT 100 GHZ

C. A. Mears, Qing Hu[a)] and P. L. Richards
Department of Physics , University of California at Berkeley, and
Materials and Chemical Sciences Division, Lawrence Berkeley Laboratory, Berkeley, CA 94720

A. H. Worsham and D. E. Prober
Department of Applied Physics, Yale University, New Haven, CT 06520-2157

A. V. Räisänen
Radio Laboratory, Helsinki University of Technology SF-02150 Espoo, Finland

Abstract

We have made accurate measurements of the noise and gain of superconducting-insulating-superconducting (SIS) mixers employing small area ($1\mu m^2$) $Ta/Ta_2O_5/Pb_{0.9}Bi_{0.1}$ tunnel junctions. We have measured an added mixer noise of 0.61 +/- 0.31 quanta at 95.0 GHz, which is within 25 percent of the quantum limit of 0.5 quanta. We have carried out a detailed comparison between theoretical predictions of the quantum theory of mixing and experimentally measured noise and gain. We used the shapes of I-V curves pumped at the upper and lower sideband frequencies to deduce values of the embedding admittances at these frequencies. Using these admittances, the mixer noise and gain predicted by quantum theory are in excellent agreement with experiment.

Introduction

Heterodyne receivers which use the nonlinear quasiparticle currents in SIS tunnel junctions have been shown to provide the lowest noise over a broad range of the millimeter and sub-millimeter electromagnetic spectrum[1,2] However, even the best of the receivers have fallen short of the performance which is predicted by the theory of quantum mixing[2,3] Because of the lack of detailed comparisons between experimental and theoretical performance, it has been unclear whether the discrepancy between measured and predicted performance is due to difficulties in coupling the signal to the mixer, or problems with the theory.

Several authors have made quantitative comparisons of SIS mixer performance with theory. Feldman et al.[4] obtained good agreement with theoretical predictions of mixer gain at 115 GHz using embedding admittances measured from a scaled model. However, they were not able to measure mixer noise accurately enough for a comparison with theory. McGrath et al.[5] made an extensive comparison between theory and experiment near 36 GHz. They concluded that the theory overestimates the gain, and underestimated the noise by a significant amount. They did not measure the embedding admittances involved in the actual experiment, and therefore could only compare experimental performance with that predicted with the embedding admittance optimized for best performance. The range of allowable embedding admittance for this work were determined from a scaled model.

In this work and more briefly in the letter that preceded it[6] we perform a detailed analysis of the performance of high quality, small area (1.0×1.0 micron) $Ta/Ta_2O_5/PbBi$ tunnel junctions used as quasiparticle mixers near 90 GHz. We compare theoretical and experimental pumped I-V curves to deduce accurate embedding admittances under experimental conditions, and use these admittances to predict both mixer noise and mixer gain. These predictions are then compared to experimentally measured values.

a) Present address: Dept. of Electrical Engineering and Computer Science and Research Laboratory of Electronics, Massachusetts Institute of Technology, Cambridge, MA 02139

Manuscript received September 24, 1990

Quantum Limit

The quantum limit for noise in linear amplifiers has been discussed by many authors. The general theoretical treatment by Caves[7] shows that any narrow-bandwidth phase-preserving linear amplifier must add noise of spectral density referred to the input of

$$S_N \geq | 1 - G_P^{-1} | \hbar\omega/2, \quad (1)$$

where G_P is the photon number gain, and ω is the angular frequency of the signal. An SIS mixer operated in the weak signal limit is linear, preserves phase, and amplifies photon number. Therefore, the above quantum limit applies. Since an SIS mixer almost always operates in the regime of large photon number gain, the quantum limit reduces to

$$S_N \geq \hbar\omega/2. \quad (2)$$

Tucker computed the noise in an SIS mixer that arises from fluctuations in the quasiparticle tunneling current.[3] This noise has the minimum value of $\hbar\omega/2$ for a single-sideband (SSB) mixer and zero for a symmetric double-sideband (DSB) mixer. This theory is incomplete in that it treats the radiation as a classical field. Wengler and Woody[8] extended the Tucker theory to the case of quantized radiation fields. They showed that the additional noise that arises from the quantization of the radiation field is $\hbar\omega/2$ for a SSB mixer, and $\hbar\omega$ for a DSB mixer. When we add these uncorrelated contributions to the noise, the minimum noise of an SIS mixer is $\hbar\omega$ for an arbitrary image termination. In this paper, we choose to consider the vacuum fluctuations incident on the mixer, as calculated by Wengler and Woody, part of the signal. This convention does not "blame" the mixer for fluctuations that were already present in the incoming signal. Thus, the quantum limit is taken to be the noise **added** by the mixer. Expressed in units of quanta, the quantum limit is 0.5 for a SSB mixer, and zero for a DSB mixer.

Experimental Details

Measurement Technique

Accurate measurements of mixer noise and gain are required in order to evaluate mixer performance . The techniques used in this work, which employed variable temperature loads, is described elsewhere.[9,10] The mixer block was a quarter-height W-band (75-110 GHz) waveguide with an adjustable non-contacting backshort.[10] Coherent radiation at the LO frequency of ~95.0 GHz was fed to the mixer through a cooled crossed-guide coupler. The 23 dB attenuation of the LO by the coupler served to isolate the mixer from room temperature thermal radiation. The straight-through arm of the coupler was terminated by a specially designed variable temperature RF waveguide load[9] which provided a calibrated blackbody signal with spectral density S_l.

The IF power P_{IF} from the mixer at 1.35 GHz was coupled to a liquid Helium temperature GaAs high electron mobility transistor (HEMT) amplifier through a quarter-wave microstrip matching transformer,[10] and then to a direct detector. A 30-dB bidirectional coupler was used to measure the reflection coefficient $|\rho|^2$ for the IF power. A cooled coaxial switch and a specially designed variable-temperature coaxial load were used to characterize the noise spectral density S_{IF} and gain-bandwidth product GB_{IF} of

the IF system.[9]

In each experiment, the appropriate parameters were optimized to maximize the coupled gain G_c.This was done by injecting a monochromatic signal through the LO waveguide at either the upper or lower sideband . This procedure maximized the output power P_{IF} of the 1.35 GHz IF system, which was monitored with a direct detector.

In each experiment, four values of the rf load temperature were chosen in the range from 1.3K to 20K, yielding four values of the input spectral density S_1. For each value of S_1, the output power at the IF frequency P_{IF} was measured. The relationship between S_1 and P_{IF} is

$$P_{IF} = GB_{IF}\left\{ S_{IF} + \rho_m^2 S_B + G_m(1-\rho_m^2)\left[S_m + S_{LO} + \alpha S_B + (1-\alpha)S_L\right]\right\}, \quad (3)$$

where G_m is the gain of the mixer, S_m, S_{LO}, and S_B are the spectral densities of the noise added by the mixer, room temperature noise leaking down the LO waveguide, and the Helium bath respectively. Here α is the loss between the rf load and the mixer, and ρ_m is the magnitude of the IF reflection from the mixer due to admittance mismatch.

Tantalum Junctions

The Ta/Ta_2O_5/PbBi junctions used for this experiment are small area (1.0 x 1.0 μm^2).[11] A 3000Å thick Ge film is thermally evaporated on the 150 µm-thick quartz substrate. 100Å of Nb and 3000Å of Ta are then ion-beam sputtered and patterned by liftoff. The thin Nb layer nucleates the bcc phase of the Ta base electrode. A chlorobenzene-soak resist process produces a 1 $(\mu m)^2$ resist "dot}" with an undercut profile necessary for lift-off. 3000Å if SiO is then thermally evaporated: lift-off of the resist "dot" defines the junction window in the SiO film. After patterning the counter-electrode lift-off stencil, the junction is ion-beam cleaned. The exposed Ta is then oxidized by a dc glow discharge in pure O_2 to produce the Ta_2O_5 tunnel barrier. Thermal evaporation of 3000Å of $Pb_{0.9}Bi_{0.1}$ and 150Å of In completes the tunnel junction. The base electrode ion-beam cleaning, oxidation, and thermal evaporation of the counter-electrode are completed in-situ in order to produce a high quality tunnel barrier. The device is completed by lift-off of the counter electrode.

The majority of the experiments reported here were carried out on a single SIS junction. This junction had a normal resistance of 72Ω at 1.3 K. Both the normal resistance and the shape of the I-V curve remained constant over a period of six months even though for much of that time the junction was stored at room temperature in a desiccator. This durability is in contrast to the behavior of earlier tantalum junctions and is attributed to the 150Å overlayer of indium deposited on top of the counter-electrode.[11]

dc I-V curves

The I-V curve of the tantalum junction used in this experiment showed an extremely sharp current rise at the sum-gap voltage as well as extremely low sub-gap leakage current. The voltage width ΔV over which the sum-gap current step rises from 0.1 to 0.9 of its full value is less than 0.01 mV. The leakage current at 0.8 V_{gap} is less than 0.05 I_c. The dc I-V curve of the junction is shown in Fig. 1.

Dependence of I-V curves on Magnetic field

The quasiparticle branches of the dc I-V curves of these junctions depended on applied magnetic field and on the amount of magnetic flux trapped in the junction. When no magnetic field was applied, and for some amount of trapped flux, the current rise at the sum-gap voltage was extremely sharp, and in some cases exhibited negative dynamic conductance. For different amounts of trapped flux, as evidenced by a lower value of the critical current, the sum-gap current rise was not so sharp, and the leakage current increased by as much as a factor of two. Two different I-V curves for the same junction at the same temperature are shown in Fig 1. Both I-V curves were measured with zero applied field.

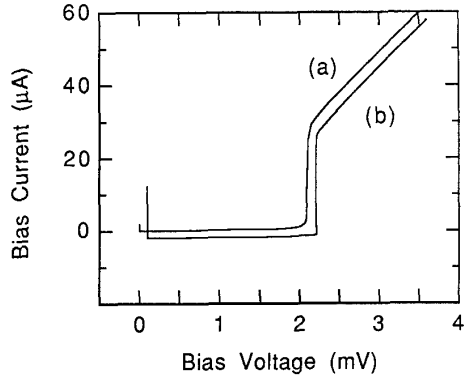

Fig. 1 Two dc I-V curves both measured in the laboratory magnetic field of approximately 1 gauss, but with different amounts of magnetic flux trapped in the junction. Note that curve (a) has a more rounded current rise at the sum gap. This curve was measuredwith more flux trapped in the junction than curve (b). Curve (b) exhibits negative dynamic conductance at the bottom end of the current rise at the sum-gap. Curve (b) is displaced diagonally from curve (a).

For the comparison between measured and calculated mixer performance discussed later in this paper, it was important that the dc I-V curve remain constant throughout the experiment. We found that certain operations, such as switching the electrically controlled coaxial switch, sent transients to the junction which caused the amount of flux trapped in the junction to change. We found that we could regain the original I-V curve by repeatedly switching the coaxial switch, presumably reproducing the original value of the trapped flux..

When an external magnetic field of moderate strength was applied parallel to the plane of the junction, the dc I-V curve changed significantly. I-V curves for the same junction at the same temperature but for several different values of the applied magnetic field are shown in Fig. 2. Notice that dynamic conductance of the sum-gap current rise decreased with increasing field, but without a significant rise in leakage current at bias voltages less than 0.8 V_g. This effect is due to a smearing of the density of states as the applied field approaches the critical field of the superconducting films.

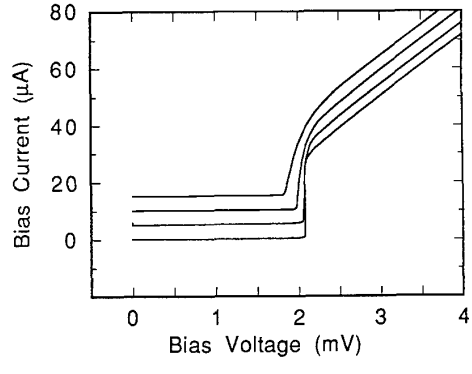

Fig. 2 A series of dc I-V curves measured with different values of the applied magnetic field. As the field is increased from zero, the density of states near the gap begins to smear out, leading to a more rounded current rise. Each curve is displaced vertically.

Mixer performance

The coupled gain and mixer noise for our mixer are plotted as a function of local oscillator frequency in Fig. 3. The backshort

position and available local oscillator power were optimized for each frequency. The minimum mixer noise was found to be 0.61 +/- 0.36 quanta at 93.0 GHz. The sideband ratio for this operating point was 9.8 dB, essentially making this a single sideband (SSB) mixer. The mixer noise is within 25 percent of the SSB quantum limit of 0.5 quanta. This is, to our knowledge, the closest approach to the quantum limit ever demonstrated.

The coupled (transducer) gain was always measured to be less than unity. Simulation has shown that DSB mixers with such sharp I-V curves can give values of coupled gain much greater than unity. We attribute our low gain to the small instantaneous bandwidth of our mixer mount at the RF frequency. This matter will be discussed in more detail later in the paper.

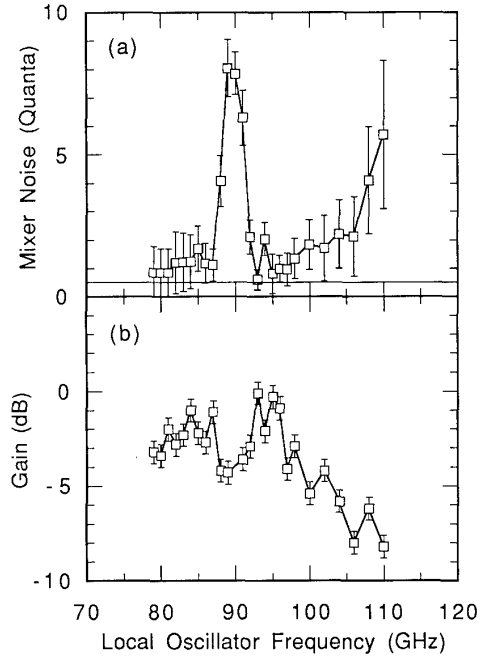

Fig. 3 Added mixer noise and available gain plotted as a function of local oscillator frequency. At each frequency, the local oscillator power, dc bias voltage and backshort position were optimized for maximum coupled gain. The peak in mixer noise near 90 GHz corresponds to a resonance in our mixer block which makes it impossible to provide favorable embedding admittances. The horizontal line at S = 1/2 is the quantum limit imposed by the uncertainty principle. The S = 1/2 vacuum fluctuations already present on the signal are not included in the mixer noise.

Comparison with Theory

In order to compare our experimental results with the Tucker theory, we have carried out computer simulations of mixer performance. All calculations were done using the three-port model, that is, with currents generated at the first and higher harmonics assumed to be short-circuited. This is a reasonable assumption in our case because the relatively large geometrical capacitance of the junction ($C \sim 160$ fF, $\omega R_N C = 14$ at 190 GHz) of the junction shunts currents at harmonic frequencies.

The Tucker theory provides a method for predicting the high frequency properties of a quasiparticle mixer from the dc I-V curve, provided that both the dc I-V curve and the rf performance are determined only by elastic tunneling processes. Because the I-V curves of our junctions closely resemble the I-V curves calculated from the BCS density of states and elastic tunneling theory, we expect that the dc I-V curve is largely determined by elastic tunneling events. Many other junctions exhibit sub-gap currents substantially in excess of those predicted by the BCS/elastic tunneling theory. These currents may not arise from elastic tunneling, and hence would not be correctly modeled by the Tucker theory. If this is the case, our junctions should be a favorable case for a quantitative test of the Tucker theory.

Determination of Embedding Admittances

To calculate mixer performance from the Tucker theory, we must know the embedding admittance at the upper sideband frequency, the lower sideband frequency, and at the intermediate frequency. These admittances can be determined in several ways. First, numerical modeling of the embedding structures could be carried out. While this may be possible in simpler situations, the complexity of our mixer block would make this process tedious and unreliable. We have instead used two other approaches. The first is to measure the admittance of a large scaled model of our mixer block at lower frequencies (3 -10 GHz) where accurate network analyzers are available. We have also determined the embedding admittance by studying the shape of the pumped I-V curve at various frequencies and backshort positions. Comparisons between these two methods show good agreement. We will now discuss numerical modeling of pumped I-V curves, and then compare the results to scale modeling results reported elsewhere.[14]

It has long been known that the embedding admittance at the pump frequency influences that shape of the pumped I-V curve.[2,3,15] We have previously given a physical explanation for this effect.[16] Other workers have used the shape of the pumped I-V curve to determine in general the range of embedding admittance provided by their mixer mounts.[17,18,19] This work utilizes the shape of the pumped I-V curve to deduce the embedding admittances needed to accurately model mixer performance.

There are several methods that can be used to determine the embedding admittance from the shape of the pumped I-V curve. In practice, these methods can be used only when shunting of harmonic response permits the use of the 3-port model. All of these methods assume an embedding admittance and an available pump power, then calculate the pumped I-V curve based on these parameters, and then compare the shape of the calculated and experimental pumped I-V curves. We outline the variations below.

These methods are similar to the method of circles first developed by Shen[17] for determining the embedding admittance from the I-V curve.

"Eyeball" Method

The first method is the so called "eyeball" technique. In this method, pumped IV curves are computed for various values of the embedding admittance, and after optimizing the available pump power, the shapes of the theoretical and experimental curves are compared by eye. This method is at best tedious and non-quantitative.

Computerized Current Match

This method is essentially an automated version of the eyeball technique. Here an admittance is assumed, the available pump power is optimized. Then the sum of the squared differences between the experimental and calculated pumped dc current is calculated for a number of representative bias voltages. The computer can be used to step through a range of admittances to find the best fit. The disadvantage of this method is that a large amount of computer time is required because a Fourier-Bessel series must be inverted for each admittance-bias point.

Computerized Voltage Match

The voltage match method[19] is a more efficient approach. In this method, the experimental pumped IV curve and the measured unpumped IV curve are used to compute the values V_k of the pump voltage at several (~10) dc voltages at which the curves are to be compared. This pump voltage is used to the compute the input admittance Y_k of the junction at the pump frequency at each of the dc voltages. For a given value of the embedding admittance Y_{LO} we can calculate a new value for each of the pump voltages using the above input admittances,

$$V'_k = \frac{I_{LO}}{Y_{LO} + Y_k} \tag{4}$$

The optimum values of the embedding admittance and the pump drive current I_{LO} are those that minimize the mean square deviation ε between the V_k's and the V_k''s,

$$\varepsilon = \sum_k (V_k - | V'_k |)^2 =$$

$$\sum_k V_k^2 + \sum_k | V'_k |^2 - 2 \sum_k V_k | V'_k | =$$

$$\sum_k V_k^2 + | I_{LO} |^2 \sum_k \frac{1}{| Y_{LO} + Y_k |^2} - \tag{5}$$

$$2 | I_{LO} | \sum_k \frac{V_k}{| Y_{LO} + Y_k |} .$$

By differentiating this expression with respect to I_{LO} we obtain the optimum value for I_{LO}, given by

$$| I_{LO} | = \frac{\sum_k \frac{V_k}{| Y_{LO} + Y_k |}}{\sum_k \frac{1}{| Y_{LO} + Y_k |^2}} . \tag{6}$$

Substituting this into the expression for ε we obtain

$$\varepsilon = \sum_k V_k^2 - \frac{\left(\sum_k \frac{V_K}{| Y_{LO} + Y_k |} \right)^2}{\sum_k \frac{1}{| Y_{LO} + Y_K |}} . \tag{7}$$

Here, ε can now be regarded as a parameter quantifying the quality of the fit between the experimental and theoretical pumped I-V curves for a given embedding admittance.

Automated Fitting

To illustrate the fitting process, we plot contour maps of the fit quality ε as a function of position on a Smith chart. An example of such a map is shown in Fig. 4. In general, when ε is less than 5 $\times 10^{-4}$ $(mV)^2$, the simulated pumped I-V curves are visually indistinguishable from each other and fit the experimental pumped IV curves very well.

Fit Quality

An example of a typical fit is shown in Fig. 5. To our knowledge, these are the highest quality fits to pumped I-V curves yet obtained. Over the past several years, we have used this procedure to fit hundreds of pumped I-V curves of various SIS junctions. In general we have found that the more closely the dc I-V curve of a given junction resembles that predicted by elastic tunneling theory, the higher the quality the fit obtained. Specifically, junctions with substantial leakage currents yield poor fits. Also, junctions whose I-V curves exhibit substantial proximity-effect induced structures immediately above the current rise at the sum-gap yield poor quality fits above the sum-gap. Typically, in such junctions, there is a region of negative dynamic conductance, and the measured dc I-V curve does not accurately represent the density of quasiparticle states near the gap because of instabilities in the bias circuit when driving this negative dynamic conductance. We have also fitted pumped I-V curves of series arrays of 5 nominally identical junctions. It has been argued[3] that such arrays can be treated as a single junction if the measured voltage and current are scaled down by a factor of five. We have found that the fits of pumped I-V curves using such a scaling procedure are of relatively poor quality, even when the junctions in the array have nearly identical critical currents.

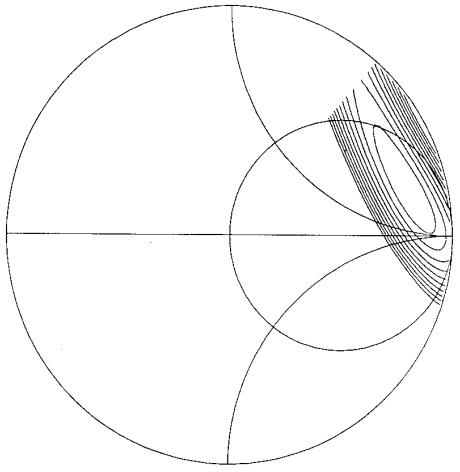

Fig. 4 Typical contour map of the fitting parameter ε as a function of embedding admittance plotted on an admittance Smith chart. Fit quality is best inside the innermost oblong contour. Within this contour calculated pumped I-V curves are visually indistinguishable from those measured experimentally. The contour spacing is 0.0005 mV^2. The chart is normalized to 0.02 Ω^{-1}.

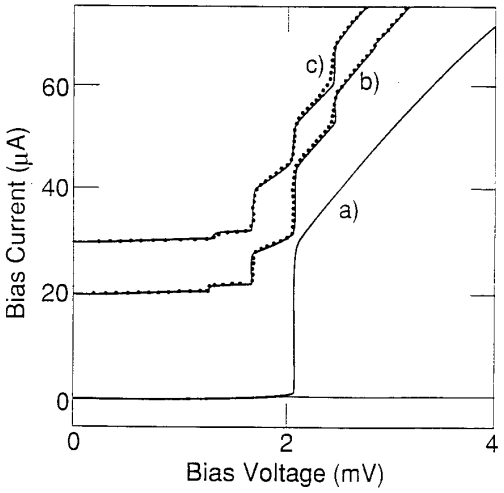

Fig.5 a) dc I-V curve of the junction studied at Temperature 1.3 K. b) Experimental and calculated pumped I-V curves. The solid line is the calculated curve. Experimental data points are represented by dots. The pump frequency was 96.35 GHz. The imbedding admittance used in the calculation was $Y = 0.14 + 0.08i\ \Omega^{-1}$. c), same as b), except that the pump frequency was 93.65 GHz and imbedding admittance was $Y = 0.04 + 0.18i\ \Omega^{-1}$. These are the upper and lower side band admittances used in the calculation of the solid lines shown in Fig. 7. All I-V curves were measured in the ambient laboratory magnetic field.

Comparison with Results from a Scaled Model

To check the validity of the I-V curve fitting technique, we can compare the deduced embedding admittances to those obtained from a scaled model. Because of experimental difficulties in our apparatus, it was difficult to relate the position of the backshort in the scaled model to the position of the backshort in the actual experiment. So, instead of comparing the deduced and measured embedding admittances for specific backshort position, we compare the range of embedding admittances accessible by moving the backshort while holding the LO frequency fixed. To do this, we measured a set of I-V curves pumped at 93 GHz, each with the backshort position stepped 0.0165mm farther away from the junction, starting at approximately 1.15mm away from the junction. The range of admittances consistent with each I-V curve was deduced using the voltage match method. For each I-V curve, this range can be represented on the Smith chart as a roughly oval shaped region. These regions, along with the range of admittance measured from the scaled model[14] at the scaled frequency, are shown in Fig. 6.

The deduced admittances are in good qualitative agreement with those measured from the scaled model. The deduced admittance fall to the outside of the range measured from the scaled model. This could be caused by inaccurate scaling, or by differences in the surface impedance between the scaled model and the mixer block at the measured frequencies. It should be noted that I-V curves were measured only for a small range of backshort positions. For most positions the admittance lies between region (a) and region (k). The pattern is qualitatively repeated with period ~ 1.5mm, which is approximately 1/2 the guide-wavelength at 93 GHz.

The successful comparison between admittances measured from a scaled model and those deduced from pumped I-V curves gives us confidence in applying the I-V curve method to the modeling of mixer performance.

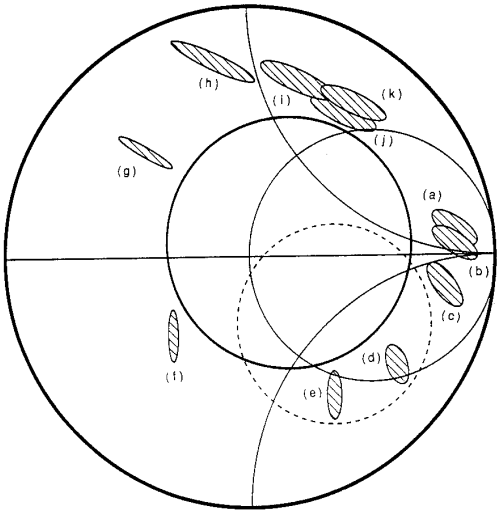

6. Range of admittances available at 93 GHz. The ranges of imbedding admittance deduced from a set of I-V curves pumped at 93 GHz, each with the backshort position stepped 0.0165mm farther away from the mixer, are represented by the shaded regions. Region (a) is for the backshort approximately 1.15mm away from the junction, with this distance increasing to region (k). The dashed circle is the range of imbedding admittances measured from the scaled model at the scaled frequency corresponding to 93 GHz. The solid circle is the same range, except that the susceptance due to the estimated capacitance of 160 fF has been added in parallel.

Simulation of Mixer Performance

We have calculated mixer performance using the Tucker theory in the 3-port approximation. We have not made the low IF approximation made by some other authors. The input data are the dc I-V curve, the bias voltage, the LO voltage amplitude V_{LO}, the rf embedding admittances Y_{usb} and Y_{lsb} at the upper and lower sideband frequencies respectively, and the IF load admittance Y_{IF}. We consider the susceptance due to the geometrical junction capacitance to be part of the embedding admittance.

To predict mixer performance we must measure or deduce the above input data under experimental conditions. The dc I-V curve and the bias voltage are straightforward to measure. The LO voltage amplitude was determined using the Tucker theory from the pumped dc current at the bias point. The IF load admittance was assumed to be matched to the mixer IF output admittance, yielding the available gain.

The RF embedding admittances were determined by pumping the mixer first at the upper sideband frequency, and then at the lower sideband frequency, and measuring a pumped I-V curve for each case. From these I-V curves, we deduced a range of embedding admittances consistent with each of these I-V curves. Ranges deduced using different available pump power were consistent. In general, the best defined ranges were obtained when the available pump power was such that the pumped dc current on the first photon-assisted-tunneling step below the sum-gap was 1/4 to 1/3 of the unpumped current immediately above the sum-gap. The admittances used in this work were deduced from I-V curves measured under these conditions.

The ranges of admittances deduced were used in the Tucker theory to predict a range of mixer performance. This was done by exhaustively sampling on a grid of admittance pairs consistent ($\varepsilon \leq 5.0 \times 10^{-4}$ $(mV)^2$) with the shape of the pumped I-V curves. The range of performance we quote was obtained by plotting a histogram of calculated available gain and mixer noise value, and noting the range into which 90 percent of the predicted values fell.

Results vs. pump power

As a first test of this procedure, we analyzed the results of a relatively simple experiment. We measured mixer noise and available gain as a function of LO power with all other parameters (i.e. LO frequency, backshort position, dc bias point, IF frequency, magnetic field, and temperature) held constant. This implies that the embedding admittances at the upper sideband and at the lower sideband were constant during the experiment, and that changes in mixer performance were due only to changes in the amplitude of the LO voltage.

In Fig. 7, we plot the experimentally measured mixer noise and available gain as a function of available pump power. The range of predicted performance consistent with the I-V curve is indicated by the dashed lines in Fig. 7. The experimental values are consistent with the predicted range of performance, but are at the poor performance end of the range. This is consistent with the conclusions reached by McGrath et al.[5] For one specific set of embedding admittances within the allowable range, we are able to predict performance that is in nearly perfect agreement with the experimentally measured values. The comparison is represented by the solid lines in Fig 7. These values of the embedding admittance are identical to those used to produce the fits to the pumped I-V curves shown in Fig. 5.

Results vs. Backshort position

We have also modeled mixer performance as function of backshort position. We measured mixer gain and noise for 13 different backshort position with LO frequency, IF frequency, and applied magnetic field held constant. The chosen positions were on either side of the optimum backshort position. At each backshort position, the LO power and dc bias point were optimized for maximum coupled gain.

The analysis of this experiment is slightly more complicated because the embedding admittance changes with backshort position. For each backshort position, we measured I-V curves pumped at the upper and lower sideband frequencies and used these to deduce ranges of allowable embedding admittances, which were used to model mixer performance. In Fig. 8 we plot the experimentally measured mixer noise and available gain as a function of backshort position. The range of predicted performance is indicated by the dashed lines in Fig. 8. The experimental values are in good agreement with the predicted range of performance for backshort

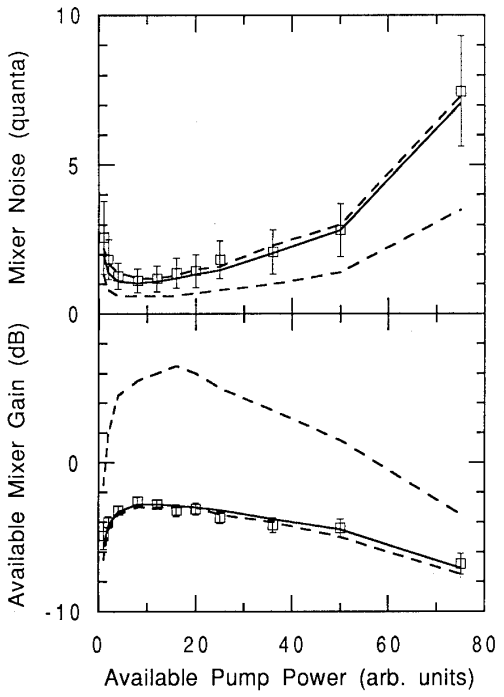

Fig. 7 Added mixer noise and available gain as a function of local oscillator power with f_{LO} = 95.0 GHz, V_{DC} = 1.956 mV. The dashed lines are the limits of the performance that are consistent with I-V curve shape. The solid line is the best fit to measured performance, with Y_{USB} = 0.14 + 0.08i Ω^{-1} and Y_{LSB} 0.04 + 0.18i Ω^{-1}. All measurements were performed with no applied magnetic field.

positions closer to the junction than 0.59mm. When the backshort is farther away, the agreement is not as good.

The admittances deduced when the backshort is farther than 0.59 mm from the junction are on the extreme outer edge of the smith chart, where either or both the real or imaginary parts of the embedding admittance is much larger than the input admittance of the junction. Under these conditions, the change of the input admittance of the junction with bias voltage does not have a large effect on the LO voltage, and hence I-V curve with different embedding admittances are quite similar. However, admittances that yield almost identical I-V curves have different values of RF reflection coefficient, and hence different mixer performance.

As the embedding admittance moves radially outward near the edge of the Smith chart, the power needed to obtain a specific pumped dc current increases rapidly. It is possible to eliminate some of the embedding admittances that are consistent with I-V curve shape, but inconsistent with the measured value of the LO power. Since the LO power is measured outside the dewar, we must know the loss between the power meter and the junction at the pump frequency. We were able to estimate this loss by using the calculated pump power for the I-V taken when the backshort is closer than 0.59mm to the junction. For these backshort positions, the embedding admittance is nearer the center of the Smith chart and the pump power varies only by a factor of two over the range of admittance consistent with I-V curve shape.

We used this procedure to restrict the range of admittances when the backshort is more than 0.59mm from the junction. In Fig. 9, we replot the experimentally measured mixer noise and available gain. The range of predicted performance calculated using the restricted range of admittances is indicated by the dashed lines. The agreement between experiment and theory is substantially improved over the range in which the corrected admittances were used. It should be noted that the performance calculated using the restricted range of admittance falls outside the range calculated using the

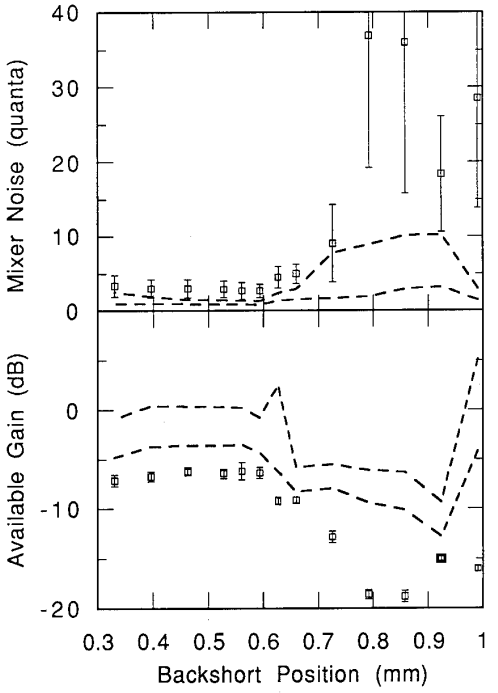

Fig. 8 Added mixer noise and available gain as a function of backshort posiiton, measured in mm from the junction. The dashed lines are the limits of performance that are consistent with I-V curve shape.

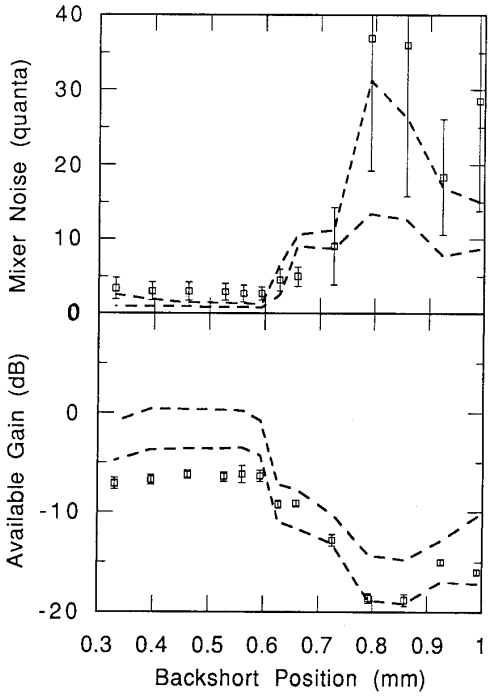

Fig. 9 Same as Fig. 8 except that now the calculated limits of performance are calculated using only admittances that are consistent with measured values of pump power for backshort position greater than 0.59mm. Note that the quality of the fit is dramatically improved in this region.

unrestricted admittances. This is because the values calculated using the restricted admittances fell outside the 90 percent range used in Fig. 8.

Discussion

It is useful to consider effects that could cause discrepancies between calculated and experimental mixer performance. It is possible that the Tucker theory overestimates the performance when the dc I-V curve is used to predict high-frequency behavior. This could occur if the dc I-V does not accurately represent the density of states. A very small negative dynamic resistance observed on the sum-gap current rise indicates that the high current density of our junctions heats the quasiparticles and sharpens the current rise at the sum-gap voltage. The time scale of this effect is much longer than one cycle of the local oscillator, so that the high frequency response is not exactly determined by the dc I-V curve. A second possibility is that the leakage current below the sum-gap does not arise from tunneling, and so is not correctly modeled by the Tucker theory. If this effect were important it could explain our relative success because the effect would be minimized in low-leakage junctions. It is possible that the determination of embedding admittance using pumped I-V curves gives incorrect results, either due to non-equilibrium phenomena, leakage currents, or other effects. We consider this unlikely because of the good agreement between the admittances deduced by the fitting procedure and those measured using a scaled model,[14] or theoretical expectations.[16]

It is also possible that harmonic effects are important for some backshort positions. This is unlikely to be the case for the first experiment where performance was measured as a function of pump power. In this experiment, the junction capacitance was nearly resonated at the LO frequency. Under these conditions, the amplitude of the RF voltage at the first harmonic of the pump frequency is ~100 times smaller than that at the pump frequency for typical pump power, and the assumptions of the three port model should be very well justified. For the second experiment, where the backshort position is varied, the embedding admittance was highly capacitive at the pump frequency when the backshort was farther than 0.59mm from the junction. Under these conditions, voltages at the first harmonic of the pump frequency could arise either from harmonic conversion in the mixer itself, or from harmonic content in the waveform of the local oscillator. The pump power needed at these backshort positions is up to 100 times larger than when the mixer is optimized, thus there is up to 100 times more power at the first harmonic frequency. It is possible that the 3-port model is no longer valid under these conditions.

We now turn the discussion to the relatively low values (less than unity) of coupled gain that we measured. Simulations have shown that junctions similar to ours can give large values of coupled gain when provided with favorable embedding admittances. The small instantaneous bandwidth of our mixer block limits our ability to simultaneously provide favorable embedding admittances at both the upper and lower side band. Simulation has shown that as the difference between the imaginary parts of the upper and lower side band embedding admittance increases, the coupled gain decreases for typical mixer parameters.[20] Coupled gain much greater than unity was measured in a full-height version of the mixer block used in this work.[21] The junction used in that experiment used an integrated tuning element to resonate the geometrical capacitance of the junction which greatly increased the instantaneous bandwidth, making the mixer almost double-sideband.

We have accurately measured the performance of an SIS mixer operating in the quantum limit where the noise is limited by the uncertainty principle. Our minimum mixer noise is a maximum of 0.42 quanta above the quantum limit for a phase-preserving linear amplifier. This is, to our knowledge, the closest approach to the quantum limit measured in any mixer. We have calculated pumped I-V curves in nearly perfect agreement with those measured in the experiment for a broad range of experimental parameters. Using admittances deduced from the fitting parameters and the Tucker theory of quantum mixing, we have predicted mixer performance in good agreement with that measured experimentally.

This work was supported in part by the Director, Office of Energy Research, Office of Basic Energy Sciences, Chemical Sciences Division of the U. S. Department of Energy under Contract No. DE-AC03-76-SF00098, and by NSF ECS-8604350 and AFOSR-88-0270. A. H. Worsham was supported in part by an IBM fellowship.

References

1. P. L. Richards and Qing Hu, "Superconducting components for infrared and millimeter-wave receivers," *Proceedings of the IEEE*, 77, 1233-1246, 1989.
2. J. R. Tucker and M. J. Feldman, "Quantum dectection at millimeter wavelengths," *Rev. Mod. Phys.*, 57, 1055-1113, 1985.
3. J. R. Tucker, "Quantum limited detection in tunnel junction mixers," *IEEE J. Quantum Electron.*, QE-15, 1234-1258, 1979.
4. M. J. Feldman, S. K. Pan, A. R. Kerr, and A. Davidson, "SIS mixer analysis using a scale model," *IEEE Trans. Magn.*, MAG-19, 494-497, 1983.
5. W. R. McGrath, P. L. Richards, D. W. Face, D. E. Prober, and F. L. Lloyd, "Accurate experimental and theoretical comparisons between superconductor-insulator-superconductor mixers showing weak and strong quantum effects," *J. Appl. Phys.* 63, 2479-2491, 1988.
6. C. A. Mears, Qing Hu, P. L. Richards, A. Worsham, D. E. Prober, and A. V. Räisänen, "Quantum limited heterodyne detection of mm waves using superconducting tantalum tunnel junctions," to be published in *Appl. Phys. Lett.*, 1990.
7. C. M. Caves, "Quantum limit on noise in linear amplifiers," *Phys. Rev. D.*,26 , 1817-1839, 1981.
8. M. J. Wengler and D. P. Woody, "Quantum noise in heterodyne detection," *IEEE J. Quantum Electron.*, QE-23, 613-622, 1987.
9. W. R. McGrath, A. V. Räisänen, and P. L. Richards, "Variable temperature loads for use in accurate noise measurements of cryogenically cooled microwave amplifiers and mixers," *Int. J. Infrared and Millimeter Waves*, 7, 543-553, 1986.
10. A. V. Räisänen, D. G. Crété , P. L. Richards, and F. L. Lloyd, "Wide-band low-noise mm wave SIS mixers with a single tuning element," *Int. J. Infrared and Millimeter Waves*, 7, 1835-1851, 1986.
11. G.-J. Cui, D. W. Face, E. K. Track, D. E. Prober, A. V. Räisänen, D. G. Crété, and P. L. Richards, "High quality Ta/PbBi tunnel junctions for 85-110 GHz SIS mixer experiments," *IEEE Trans. Magn.*, MAG-23, 688-691, 1987.
12. M. Hatzakis, B. J. Canavello, and J. M. Shaw,"Single step optical lift-off process", *IBM J. Res. Dev.*, 24, 452-460, 1980.
13. S. Raider, private communication.
14. A. V. Raisanen. W. R. McGrath, D. G. Crété, and P. L. Richards, "Scaled model measurements of embedding impedances for SIS waveguide mixers," *Int. J. Infrared and Millimeter Waves*, 6, 1169- 1189, 1985.
15. Qing Hu, C. A. Mears, P. L. Richards, and F. L. Lloyd, "Quantum susceptance and its effects on the high frequency response of superconducting tunnel junctions," to be published in Phys. Rev. B, 1990.
16. C. A. Mears, Qing Hu, and P. L. Richards, "Numerical simulation on experimental data from planar SIS mixers with integrated tuning elements," *IEEE Trans. Magn.*, MAG-25, 1050-1053, 1989.
17. T. M. Shen, "Conversion gain in millimeter wave quasiparticle heterodyne mixers," *IEEE J. of Quantum Electron.*, QE-17, 1151-1165, 1981.
18. T. G. Phillips and G. J. Dolan, " SIS mixers," *Physica* , 109 and 110B, 2010-2019, 1982.
19. Anders Skalare, "Determining embedding circuit parameters from dc measurements on quasiparticle mixers," *Int. J. of Infrared and Millimeter Waves*, 10, 1339-1353, 1989.
20. C. A. Mears, unpublished.
21. A. V. Räisänen, D. G. Crété, F. L. Lloyd, and P. L. Richards, "A 100-GHz quasiparticle mixer with 10 dB coupled gain," *IEEE MTT-S Dig.*, 929-930, 1987.